

Synthesis and High-Resolution NMR Structure of a β^3 -Octapeptide with and without a Tether Introduced by Olefin Metathesis

by Marc-Olivier Ebert^{*a)}, James Gardiner^{a)b)c)}, Steven Ballet^{b)d)}, Andrew D. Abell^{*b)}, and Dieter Seebach^{a)}

^{a)} Laboratory of Organic Chemistry, Department of Chemistry and Applied Biosciences, ETH Zürich, HCI Hönggerberg, Wolfgang-Pauli-Strasse 10, CH-8093 Zürich
(phone: +41-44-633-4726; e-mail: marc-olivier.ebert@org.chem.ethz.ch)

^{b)} School of Chemistry and Physics, University of Adelaide, Adelaide 5000, Australia
(phone: +61-8-8303-5652; fax: +61-8-8303-4358; e-mail: andrew.abell@adelaide.edu.au)

^{c)} Bio21 Institute, University of Melbourne, Melbourne 3010, Australia

^{d)} Department of Organic Chemistry, Vrije Universiteit Brussel, Pleinlaan 2, B-1050 Brussel

Bridging between (*i*)- and (*i*+3)-positions in a β^3 -peptide with a tether of appropriate length is expected to prevent the corresponding 3_{14} -helix from unfolding (Fig. 1). The β^3 -peptide H- β^3 hVal- β^3 hLys- β^3 hSer(All)- β^3 hPhe- β^3 hGlu- β^3 hSer(All)- β^3 hTyr- β^3 hIle-OH (**1**; with allylated β^3 hSer residues in 3- and 6-position), and three tethered β^3 -peptides **2–4** (related to **1** through ring-closing metathesis) have been synthesized (solid-phase coupling, Fmoc strategy, on chlorotriptyl resin; Scheme). A comparative CD analysis of the tethered β^3 -peptide **4** and its non-tethered analogue **1** suggests that helical propensity is significantly enhanced (threefold CD intensity) by a (CH₂)₄ linker between the β^3 hSer side chains (Fig. 2). This conclusion is based on the premise that the intensity of the negative Cotton effect near 215 nm in the CD spectra of β^3 -peptides represents a measure of 'helical content'. An NMR analysis in CD₃OH of the two β^3 -octapeptide derivatives without (i.e., **1**) and with tether (i.e., **4**; Tables 1–6, and Figs. 4 and 5) provided structures of a degree of precision (by including the complete set of side chain–side chain and side chain–backbone NOEs) which is unrivaled in β -peptide NMR-solution-structure determination. Comparison of the two structures (Fig. 5) reveals small differences in side-chain arrangements (separate bundles of the ten lowest-energy structures of **1** and **4**, Fig. 5, A and B) with little deviation between the two backbones (superposition of all structures of **1** and **4**, Fig. 5, C). Thus, the incorporation of a CH₂–O–(CH₂)₄–O–CH₂ linker between the backbone of the β^3 -amino acids in 3- and 6-position (as in **4**) does accurately constrain the peptide into a 3_{14} -helix. The NMR analysis, however, does not suggest an increase in the population of a 3_{14} -helical backbone conformation by this linkage. Possible reasons for the discrepancy between the conclusion from the CD spectra and from the NMR analysis are discussed.

1. Introduction. – β -Peptides, oligomers composed of homologated proteinogenic amino acids, have received considerable attention for their ability to adopt rather stable and predictable conformations in solution [1a]¹⁾. One of the most common, and most

¹⁾ As compared to α -amino acids, the homologated proteinogenic amino acids have an additional rotatable C–C bond. This is in contrast to the situation in *trans*-2-aminocyclopentane and -cyclohexane carboxylic acids (originally studied by Gellman and co-workers [1b]); the cyclohexane (and the 1,2-dithiane [1c]) amino-carboxylic-acid moiety is actually the strongest 3_{14} -helix-stabilizing unit in β -peptides [1d] (an inversion of the six-membered-ring chair conformation with equatorial CONH and NHCO moieties would put these substituents and the attached chains in axial positions!).

studied, conformations is that of the 3_{14} -helix, where β -peptides composed of six or more β^3 -amino-acid residues fold in solution to a regular helical structure stabilized by 14-membered H-bonded rings with approximately three residues per helix turn. Such structures have found interest not only in their own right, but also for their ability to interact with proteins and receptors and to display biological activity (for general reviews on β -peptides, see [2]).

As such, the stabilization of β -peptidic 3_{14} -helices, particularly in aqueous solutions, has offered a challenge in recent times. For α -peptides, helix stabilization has been achieved using a number of different strategies (for recent reviews on α -helix stabilization, see [3]). The most common of these involves the covalent linking of adjacent turns of the helix by means of constraints between amino acid side chains (*i.e.*, disulfides, lactams [4], triazoles [5], and C-tethers *via* ring-closing metathesis (RCM) [6–8]), or the replacement of weak H-bonds with alkyl or hydrazone bridges [9].

Early work on β -peptidic 3_{14} -helices showed that helix stabilization could be accomplished through the incorporation of cyclic β -amino acids [1b,c][2d][10] or strategically placed salt bridges [11]²). Incorporation of a disulfide linkage, common in α -peptides, between the β^3 -cysteine residues in i and $i+3$ positions of a 3_{14} -helix was also investigated, and represented the first example of a covalent constraint used in the stabilization of 3_{14} -helical β -peptides [12] (*Fig. 1*). Recently, *Vaz* and *Brunsveld* have shown that the covalent linking of β -amino acid residues at i and $i+3$ positions *via* an amide bond results in β -peptides with a high degree of 3_{14} -helicity in H₂O, as concluded from CD spectra [13] and from a number of typical [1a][2c] nuclear *Overhauser* effects (NOEs) observed in the NMR spectra [1d].

Here, we describe the first detailed NMR solution-structure analysis of a constrained 3_{14} -helical β^3 -peptide (prepared through RCM), including a comparison with the NMR structure of its non-constrained analog, and we compare the results of the NMR analysis with conclusions from CD spectra.

2. Design and Synthesis of the i -to- $(i+3)$ -Bridged β -Peptides 2–4, and of the Linear Analog 1. – β^3 -Octapeptides **1–4** (*Scheme*) are designed to adopt a 3_{14} -helix in solution. The β -amino-acid sequence contains several features promoting helical stability: *i*) it consists of β^3 -amino acids that are known to adopt particularly stable helical structures [1][2][11]; *ii*) a β hLys residue at position 2 and a β hGlu residue at position 5 provide potential for salt-bridge formation in a 3_{14} -helix; *iii*) a β hPhe residue at position 4 and a β hTyr residue at position 7 provide potential for aromatic π/π interaction; *iv*) finally, and most importantly, peptides **2**, **3**, and **4**, contain a covalent C-bridge between β hSer residues at positions 3 and 6 (giving a 21-membered heterocycle) to prevent unfolding of the helix (*cf. Fig. 1*)³). The β^3 -octamers **1–4** allow

2) Multiple salt bridging, ‘capping’ of the macrodipole, and introducing amphipathic character of 3_{14} - β -peptidic helices by *Schepartz* and co-workers led to helix stability in H₂O and aggregation to protein-type quaternary structures [11c–h].

3) The thus tethered β -peptide happens to contain a macrocycle of the same ring size (21 atoms) as that in the β -peptide with an amide bond between (i) - and $(i+3)$ -positioned β hLys and β hGlu residues [1d][13], while in the β -peptide with a disulfide bridge, shown in *Fig. 1* [12], the macrocycle contains only 17 atoms.

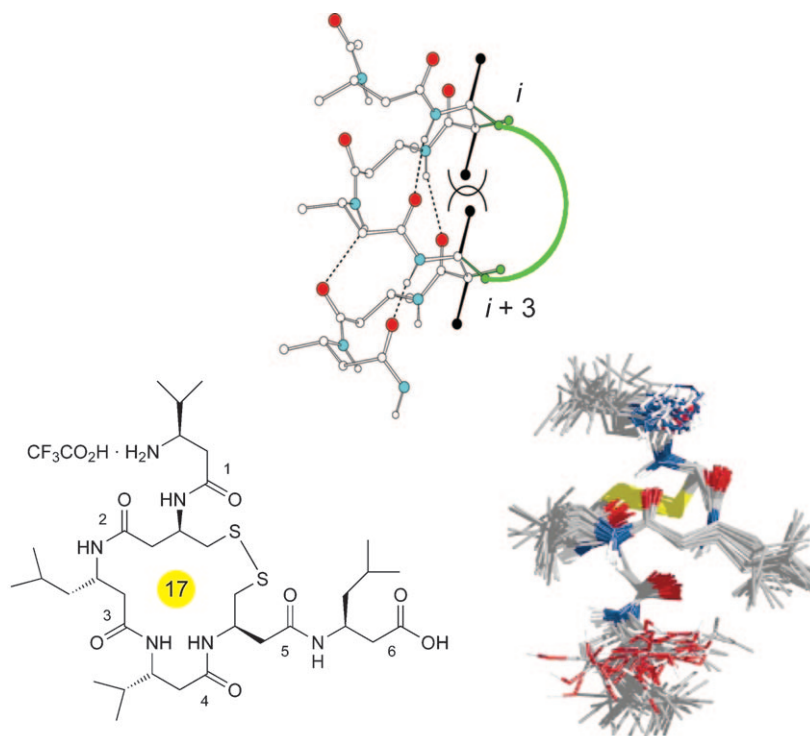


Fig. 1. Juxtaposition of substituents in i - and $(i + 3)$ -position of a β -peptidic (M)- 3_{14} -helix and disulfide bridging between these positions in a β^3 -hexapeptide [12]

for two complete turns of a 3_{14} -helix (with up to seven intramolecular H-bonds [1a][2c]).

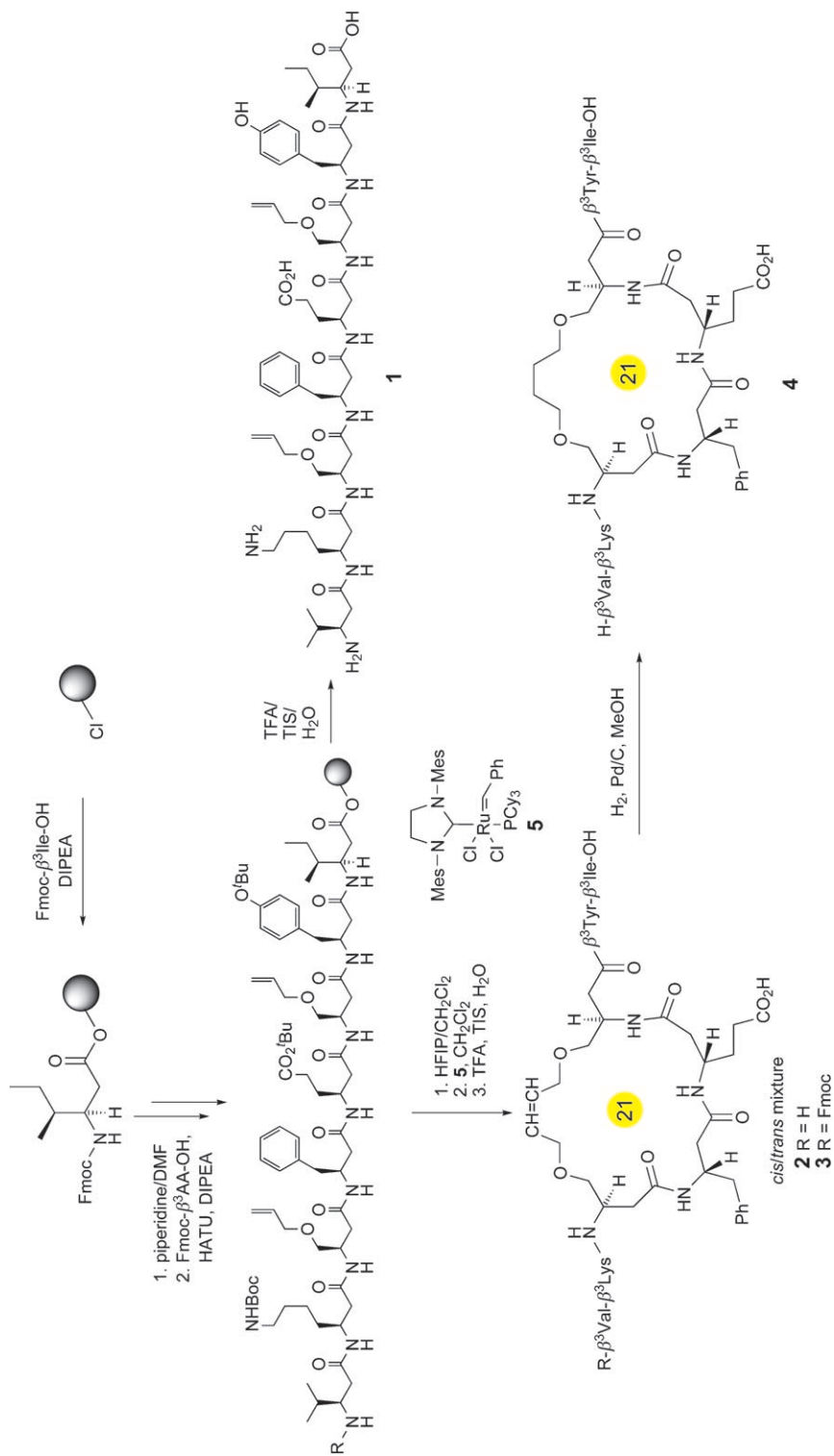
The synthesis of the peptides **1**–**4** involved an on-bead strategy with incorporation of two O -allyl- β^3 hSer residues [14] for subsequent RCM (*Scheme*). Removal of the on-bead assembled peptide from the resin with simultaneous deprotection of the side-chain protecting groups under standard conditions gave the linear β^3 -octapeptide derivative **1**.

Initial efforts to carry out RCM ‘on-resin’ proved unsuccessful⁴⁾. Instead, the fully side-chain-protected linear peptides were cleaved from the resin under mild acidic conditions (HFIP, CH_2Cl_2) affording compounds soluble in organic solvents. Ring closing metathesis proceeded smoothly in the presence of *Grubbs* II ruthenium catalyst **5** in CH_2Cl_2 , to give the tethered peptides **2** and **3** as predominantly the (*E*)-isomers (ratio *ca.* 4 : 1 by $^1\text{H-NMR}$). Removal of the side-chain protecting groups under acidic conditions gave the $\text{CH}_2\text{CH}=\text{CHCH}_2$ -tethered peptide **2** (or its *N*-terminal Fmoc derivative **3**)⁵⁾ in good yield. Subsequent hydrogenation of **2** provided the β^3 -

4) In this case, it was only possible to explore variations in thermal conditions. For examples, where microwave conditions have been successfully employed in this regard, see [8].

5) The Fmoc derivative was initially prepared to allow for adequate detection of the peptide by UV during HPLC analysis and purification.

Scheme. Synthesis of the Linear β -Octapeptide **1** and of the Tethered β -Peptides **2–4**, Using a Ring-Closing Metathesis (RCM) Approach. For abbreviations, see General in the Exper. Part.



octapeptide **4** with a C₄ alkyl-chain tether between the β³hSer residues at positions 3 and 6. Preparative RP-HPLC purification produced samples of **1–4** with purities > 98%.

3. CD Analysis of the β³-Octapeptides with and without Tether. – With purified material in hand, we first used circular dichroism (CD) spectroscopy to analyze the ‘helical content’ of the linear β-peptide **1** (containing two O-allyl-β³hSer residues) and the tethered β-peptide analogue **4** at 25°, in MeOH, and also in H₂O (Fig. 2). The CD spectra of **1** and **4** in MeOH (Fig. 2, a) show curves characteristic of ₃1₄-helices [2c], i.e., minima at or near 215 nm, maxima between 195 and 205 nm, and a crossover from positive to negative ellipticity between 205 and 210 nm. The mean ellipticity minimum displayed by linear β-peptide **1** (–10000) in MeOH is consistent with that of similar linear β-peptides analyzed in the past [1][2][11–13]. A significant increase in the negative Cotton effect is seen for the tethered analogue **4** (ca. –25000, almost threefold that of **1**), indicating enhanced helical propensity in MeOH as a result of the covalently linked β³hSer residues. Significantly, this enhanced effect is also apparent in H₂O with maximum negative mean molar ellipticities of –5000 and –15000 observed for **1** and **4**, respectively. Based on the assumption that a correlation exists between intensity of the negative Cotton effect near 215 nm and the ₃1₄-helical propensity of a β³-peptide⁶⁾, we conclude that **4** displays an enhanced helical propensity in MeOH, and especially in H₂O. The observed effect of (CH₂)₄-tethering on the CD spectra compares favorably with that of the β-peptides tethered with an amide linker [1d][13].

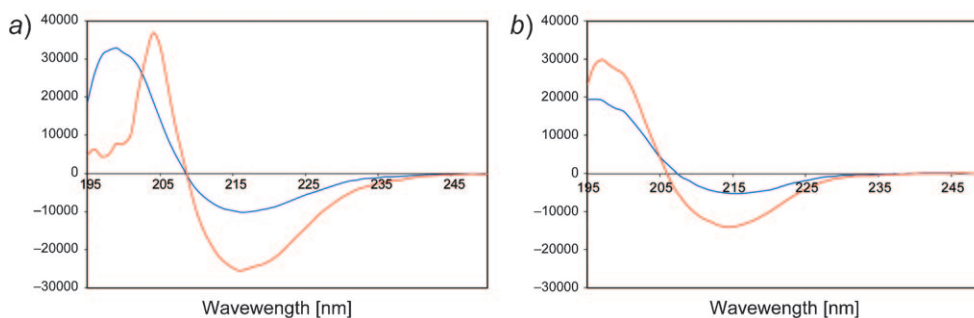


Fig. 2. Normalized CD spectra of the linear β-peptide **1** (blue) and the tethered β-peptide **4** (red) in MeOH (a), and in H₂O (b; pH 7.1)

In summary, CD analysis of **4** suggests a significant increase in ₃1₄-‘helical content’, in both organic and aqueous solution, as a result of the incorporation of an alkane tether. To further examine the influence of this tether on the conformation of the ₃1₄-helix, a detailed NMR-solution analysis of peptides **1** and **4** was carried out. A

⁶⁾ In our experience, CD-only analysis of β-peptides can be grossly misleading; we have observed ‘typical helix-indicating’ CD spectra of β-peptides, which cannot possibly fold to ₃1₄-helices [2c][15]. For a scholarly discussion of helical conformational manifolds and helical propensities of α- and β-peptides, see [16].

qualitative NMR analysis (NOE effects) was also performed with the *cis/trans*-mixture **3**, indicating that these stereoisomers also fold to a 3_{14} -helix in MeOH⁷⁾.

4. NMR Solution Structures of **1 and **4**.** – Two NMR samples were prepared by dissolving 5 mg of **1** or **4** in 700 μ l of CD₃OH to give 6 mM solutions of the β -octapeptides. Sequence-specific assignments of the ¹H- and ¹³C-resonances were accomplished by COSY, TOCSY, HSQC, and HMBC. Assignments for **1** and **4** are listed in *Tables 1* and 2. The atom-designation scheme used is illustrated in *Fig. 3*.

Table 1. The ¹H- and ¹³C-NMR Chemical Shifts of **1** in CD₃OH Referenced to Internal TMS

	HN	H _{Si,Re} ^g	H ^{β}	H ^{γ} (^a)	H ^{δ}	H ^{δ} (^{1a}) ^{b)}	H ^{δ} 2	H ^{ϵ} (^a)	H ^{ξ}	H _{Z,E} ^{ν}	H ^{ζ}
β^3 hVal ¹	–	2.65, 2.82	3.42	2	–	1.08	1.06	–	–	–	–
β^3 hLys ²	8.18	2.47, 2.87	4.49	1.59*(^c), 1.53	1.44	–	–	1.71, 1.65	2.91	–	n.o. ^{d)}
β^3 hSer ³	8.55	2.42, 2.72	4.35	3.41, 3.33	–	–	–	3.98	–	5.15, 5.25	5.86
β^3 hPhe ⁴	8.54	2.43, 2.81	4.56	2.87, 2.76	–	–	–	7.16	7.26	–	7.21
β^3 hGlu ⁵	8.23	2.44, 2.62	4.39	1.84*, 1.71	2.24	–	–	–	–	–	–
β^3 hSer ⁶	7.8	2.61, 2.39	4.62	3.46, 3.35	–	–	–	3.99	–	5.15, 5.25	5.88
β^3 hTyr ⁷	7.75	2.56, 2.34	4.69	2.72	–	–	–	7.02	6.62	–	–
β^3 hIle ⁸	7.71	2.57, 2.36	4.24	1.48	–	1.47, 1.10	0.89	0.88	–	–	–

	C ^{α}	C ^{β}	C ^{γ}	C ^{δ}	C ^{δ} (^{1b})	C ^{δ} 2	C ^{ϵ}	C ^{ξ}	C ^{ν}	C ^{ζ}	C
β^3 hVal ¹	36.9	57.0	32.3	–	19.7	19.0	–	–	–	–	172.5
β^3 hLys ²	42.1	47.5	36.3	24.1	–	–	28.5	41.0	–	–	174.0
β^3 hSer ³	38.9	47.5	73.1	–	–	–	73.2	–	117.4	136.2	172.2
β^3 hPhe ⁴	41.5	49.5	43.5	139.7	–	–	130.7	129.6	–	127.7	172.6
β^3 hGlu ⁵	41.7	47.5	32.8	32.8	–	–	177.4	–	–	–	171.9
β^3 hSer ⁶	38.9	47.8	73.2	–	–	–	73.3	–	117.4	136.2	171.6
β^3 hTyr ⁷	41.2	49.2	42.0	130.0	–	–	131.8	116.5	–	157.3	171.8
β^3 hIle ⁸	38.2	52.6	40.8	–	26.8	15.6	12.3	–	–	–	177.2

^a) Tabulated from lower to higher field. ^b) Val: C ^{δ} 1 = C ^{δ} _{Si}. ^c) * refers to H_{Si} ^{ν} . ^d) n.o. = Not observed.

For both β -peptides, stereospecific assignments were possible for the H-atoms attached to C ^{α} (all residues), the Me groups of β^3 hVal¹, and the H-atoms at γ positions in residues 2 and 5. With exception of the constitutionally different parts in residues 3 and 6, the two β -peptides show remarkably similar ¹H- and ¹³C-NMR chemical shifts.

Distance restraints for the structure calculations were generated using ROESY spectra with 300 ms mixing time resulting in 113 ROE restraints for β -peptide **1** and 102 ROE restraints for β -peptide **4**. H-Bond restraints were not included in the calculation.

The ³J values between the amide H-atom and the H-atom at β -position were used as additional restraints. The ³J(HN,H ^{β}) value for residues 2–8 lies between 8.2 and 9.7 Hz in both β -peptides (see *Table 3*). According to the *Karplus* relation published by *Wang* and *Bax* [17] for the corresponding dihedral angle in proteins, these values match a backbone dihedral angle ϕ of $-120 \pm 30^\circ$ (see *Fig. 4* for the definition of the dihedral

7) We thank Professor *B. Jaun* for sharing these unpublished results with us.

Table 2. The ^1H and ^{13}C -NMR Chemical Shifts of **4** in CD_3OH Referenced to Internal TMS

	HN	$\text{H}_{\text{Si},\text{Re}}^{\zeta}$	H^{β}	$\text{H}^{\gamma(\text{a})}$	H^{δ}	$\text{H}^{\delta(\text{1a})\text{b)}$	$\text{H}^{\delta 2}$	$\text{H}^{\varepsilon(\text{a})}$	H^{ζ}	$\text{H}^{\zeta(\text{a})}$
$\beta^3\text{hVal}^1$	–	2.6, 2.90	3.43	2.03	–	1.08	1.07	–	–	–
$\beta^3\text{hLys}^2$	8.23	2.4, 3.00	4.50	1.59 ^(*) , 1.49	1.44	–	–	1.70, 1.64	2.91	n.o. ^(d)
$\beta^3\text{hSer}^3$	8.24	2.15, 2.94	4.30	3.61, 3.31	–	–	–	3.54, 3.36	–	1.81, 1.54
$\beta^3\text{hPhe}^4$	8.47	2.421, 2.83	4.61	2.87, 2.78	–	–	–	7.18	7.26	7.20
$\beta^3\text{hGlu}^5$	8.30	2.40, 2.61	4.34	1.83 ^(*) , 1.69	2.23	–	–	–	–	–
$\beta^3\text{hSer}^6$	8.06	2.71, 2.32	4.63	3.40, 3.33	–	–	–	3.63, 3.57	–	1.82, 1.53
$\beta^3\text{hTyr}^7$	7.68	2.54, 2.33	4.67	2.74, 2.72	–	–	–	7.02	6.62	–
$\beta^3\text{hIle}^8$	7.61	2.52, 2.29	4.27	1.48	–	1.48, 1.11	0.89	0.90	–	–
	C^{α}	C^{β}	C^{γ}	C^{δ}	$\text{C}^{\delta(\text{1b})}$	$\text{C}^{\delta 2}$	C^{ε}	C^{ζ}	C^{ζ}	C
$\beta^3\text{hVal}^1$	36.6	56.9	32.3	–	19.6	18.8	–	–	–	172.6
$\beta^3\text{hLys}^2$	41.8	47.5	36.6	24.2	–	–	28.6	41.0	–	174.0
$\beta^3\text{hSer}^3$	38.7	48.7	74.6	–	–	–	73.4	–	27.8	172.2
$\beta^3\text{hPhe}^4$	41.2	49.5	43.5	139.8	–	–	130.8	129.6	127.7	172.5
$\beta^3\text{hGlu}^5$	42.1	47.6	32.9	33.1	–	–	177.9	–	–	171.9
$\beta^3\text{hSer}^6$	38.9	47.0	73.0	–	–	–	72.3	–	28.4	171.9
$\beta^3\text{hTyr}^7$	41.5	49.5	42.1	129.9	–	–	131.9	116.5	157.3	171.8
$\beta^3\text{hIle}^8$	39.1	53.0	41.0	–	26.9	15.6	12.3	–	–	178.1

a) Tabulated from lower to higher field. b) Val: $\text{C}^{\delta 1} = \text{C}_{\text{Si}}^{\delta}$. c) * refers to $\text{H}_{\text{Si}}^{\gamma}$. d) n.o. = Not observed.

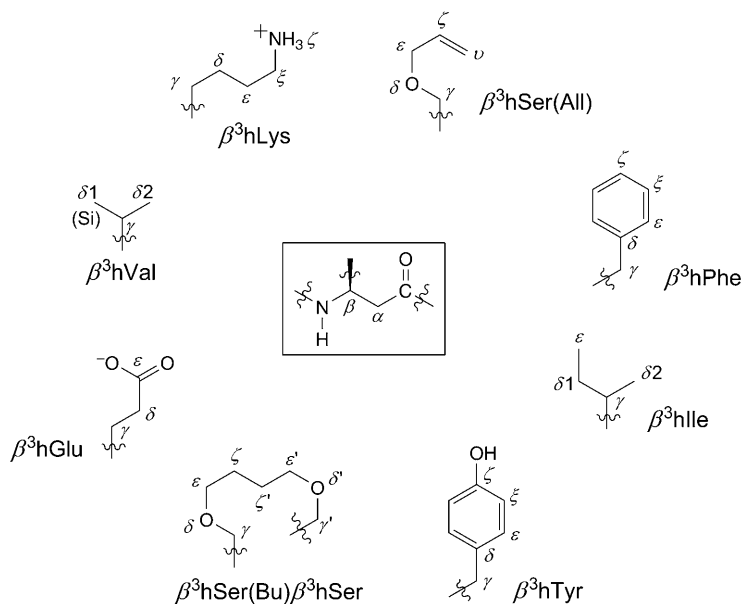


Fig. 3. $\beta^3\text{h}$ -Amino acid atom-designation scheme used for the assignment of chemical shifts and the definition of dihedral angles (cf. Fig. 4)

angles). In the structure calculations of β -peptides **1** and **4**, the dihedral angle ϕ in residues 2–8 was restrained to a more generous region of $-120 \pm 40^\circ$.

Table 3. $^3J(HN,H\beta)$ Values [Hz] Determined for β -Octapeptides **1** and **4**

	1	4
β^3hVal^1	–	–
β^3hLys^2	9.5	9.3
β^3hSer^3	8.8	8.2
β^3hPhe^4	9.4	9.7
β^3hGlu^5	9.1	8.9
β^3hSer^6	8.5	8.6
β^3hTyr^7	9.2	8.9
β^3hIle^8	9.2	9.3

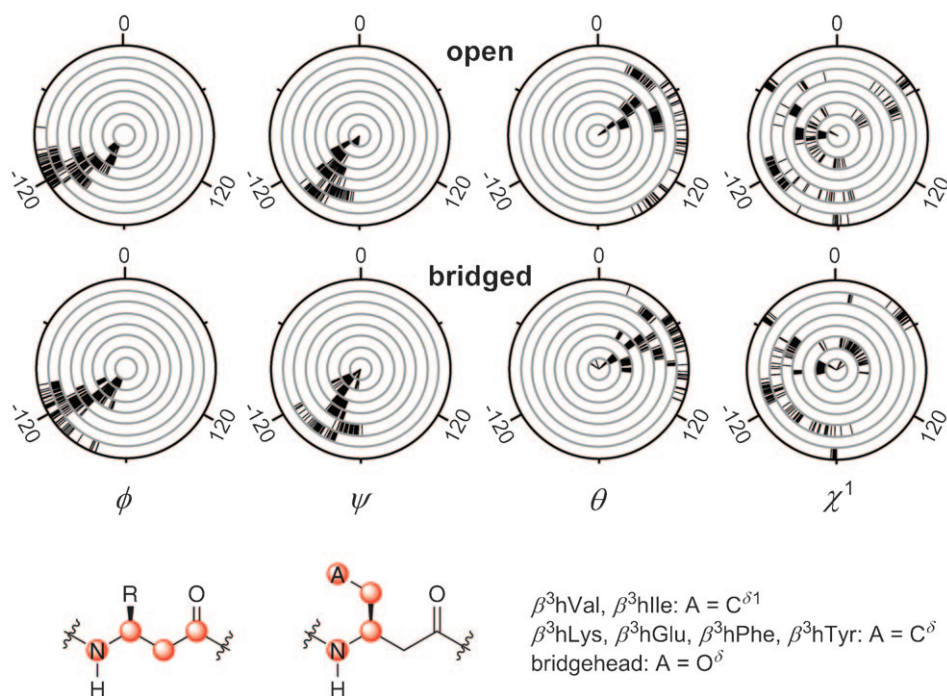


Fig. 4. Dihedral-angle distribution in the accepted structures. Top row: dihedral angles in the 45 accepted structures of β^3 -octapeptide **1**. Bottom row: dihedral angles in the 45 accepted structures of β^3 -octapeptide **4**. The innermost circle of each dial shows the dihedral angles of the first residue in the sequence (if defined). The adjacent rings show the dihedral angles of residues 2–8 (if defined). Each tick corresponds to one structure. The definitions of the dihedral angles are shown at the bottom of the figure.

Using a simulated annealing protocol, 45 structures for each molecule were calculated by restrained molecular dynamics. The statistics of the structure calculations are listed in Table 4. The backbone RMSD of helix **1** (0.16 Å) is not significantly higher

Table 4. *Statistics of the Accepted Structures of β -Octapeptides **1** and **4** in the Simulated Annealing Calculations.* Of the 45 calculated structures for each peptide, all met the acceptance criteria described in the *Exper. Part*.

	4	1
Number of NOE restraints	102	113
Intraresidual	60	70
Sequential	14	11
Others	28	32
Number of dihedral angle restraints	7	7
RMSD from experimental restraints		
Distance restraints [\AA]	0.011 ± 0.006	0.01 ± 0.001
Dihedral angle restraints [$^\circ$]	0.005 ± 0.01	0.0002 ± 0.0009
RMSD from holonomic restraints (force field)		
Bonds [\AA]	0.001 ± 0.0003	0.001 ± 0.0001
Bond angles [$^\circ$]	0.14 ± 0.04	0.3 ± 0.007
Improper [$^\circ$]	0.16 ± 0.009	0.14 ± 0.004
Atomic RMSD (residues 2–7) [\AA] ^{a)}	0.15	0.16

^{a)} Superposition was carried out over backbone atoms N, C, C $^\alpha$, and C $^\beta$ of residues 2–7.

than that of its ‘stabilized analogue’ **4**. *Fig. 5 (A and B)* depicts separate bundles of the ten lowest-energy structures of **1** and **4**, respectively, where both sequences form well-defined 3_{14} -helices. The good definition of both backbones is reflected in the backbone dihedral angle distributions shown in *Fig. 4* and listed in *Tables 5* and *6*. The backbone dihedral angles ϕ , ψ , and θ of residues 2–7 show a RMSD of $< 10^\circ$ for all (for **1**) or most of the residues (for **4**).

The β^3 -octapeptides **1** and **4** are potentially able to form six backbone–backbone H-bonds from HN_i to CO_{i+2} . If we define criteria for the existence of a $\text{NH}\cdots\text{OC}$ H-bond to be a maximal $\text{H}\cdots\text{O}$ separation of 2.4 \AA and a deviation from $\text{NH}\cdots\text{O}$ linearity of less than 35° , then each of the inner four H-bonds is observed at least eight times within the ten structures of both **1** and **4** shown in *Fig. 5, A and B*. Within the same subset of the calculated structures, the terminal H-bond from HN^6 to CO^8 is observed eight times for **1** and four times for **4**. The H-bond from HN^1 to CO^3 is absent in the ten lowest-energy structures of **4** and observed only twice within the ten structures of **1** shown in *Fig. 5, A*. Using the same criteria, the potential salt bridge between the side chains of $\beta^3\text{hLys}^2$ and $\beta^3\text{hGlu}^5$ was identified twice within the bundle of **4** shown in *Fig. 5, B*, but is absent in the structures of **1** in *Fig. 5, A*.

The position of the side chains is defined fairly well in both structures, with only the side chains of residues 3 and 6 in the non-tethered β -peptide **1** showing increased positional variability. This is also apparent in the RMSDs of the side-chain dihedral angle χ^1 of $\beta^3\text{hSer}^3$ and $\beta^3\text{hSer}^6$ in **1** (*Table 5*), which show – with the only exception of χ^1 of $\beta^3\text{hIle}^8$ – by far the highest values among the dihedral angles listed for both β -peptides. This is, however, presumably due to a lack of unambiguous distance restraints for the side-chain H-atoms of these residues and does not necessarily reflect a real increase in conformational mobility within these regions.

In *Fig. 5, C*, a backbone superposition is shown of all calculated structures of the two β -peptide derivatives **1** and **4**. The RMSD for this superposition is 0.21 \AA . This

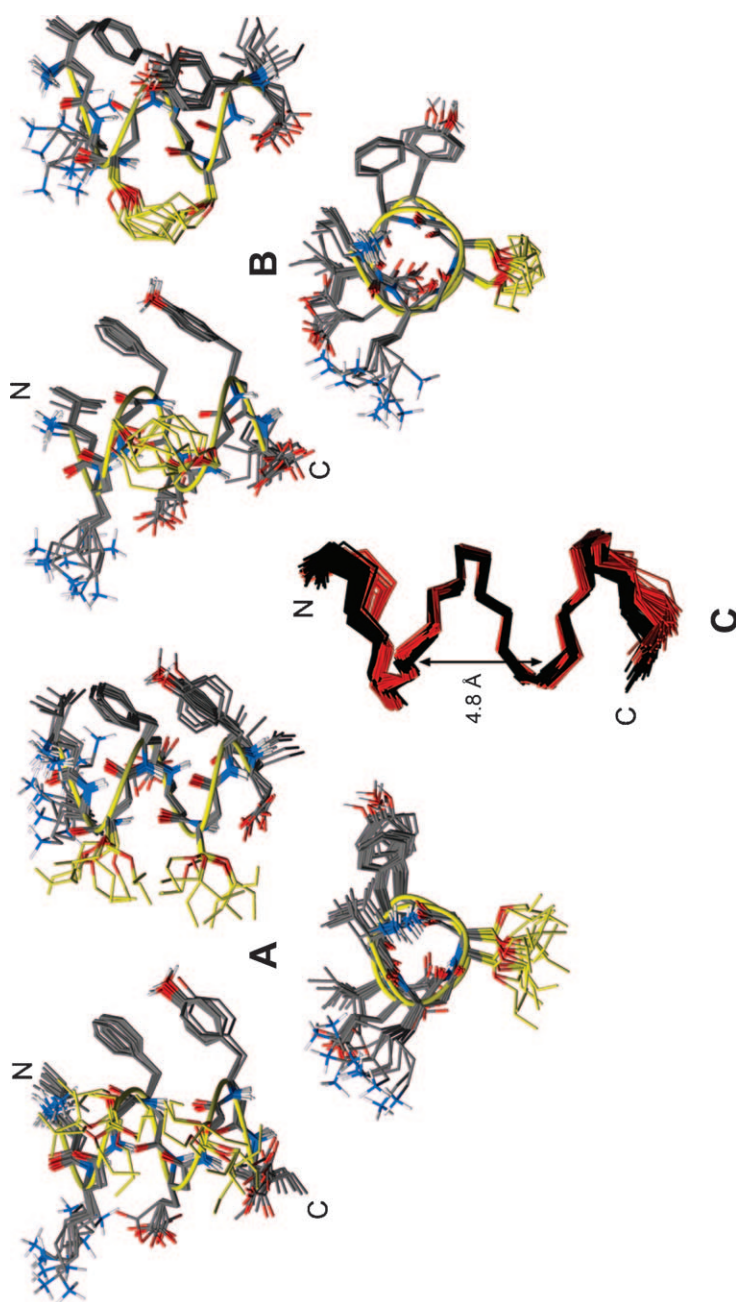


Fig. 5. Superposition of the structures of β -octapeptides **1** and **4**. **A** and **B**: The ten lowest-energy structures of **1** and **4**. Superposition was carried out over backbone atoms N, C, C^α, and C^β of residues 2–7. Each bundle is shown from three different perspectives (front view, side view (rotated by 60°), and top view). In each bundle, a yellow ribbon through atoms C^β in residues 1–8 of the structure lowest in energy indicates the backbone of the 3_{14} -helix. The side chains of residues 3 and 6 (β^3 hSer(All) in **1** and bridge in **4**) are also colored yellow. C- and N-termini of the sequences are indicated by the letters C and N. **C**: Superposition of all 45 structures of **1** and of **4** (red). Superposition was carried out over atoms N, C, C^α, and C^β of residues 2–7. Only the backbone is shown. The average C^β...C^β distance within the helices is ca. 4.8 Å (pitch of the helix).

Table 5. *Statistics of Selected Dihedral Angles in the Structural Ensemble Calculated for β -Octapeptide 1.*
All 45 accepted structures were used. For definitions of dihedral angles, see Fig. 4.

	ϕ	ψ	θ	χ^1
$\beta^3\text{hVal}^1$	–	-152 ± 9	56 ± 4	-63 ± 2
$\beta^3\text{hLys}^2$	-139 ± 7	-120 ± 3	52 ± 3	-85 ± 7
$\beta^3\text{hSer}^3$	-153 ± 4	-132 ± 8	66 ± 5	-107 ± 52
$\beta^3\text{hPhe}^4$	-139 ± 9	-145 ± 7	48 ± 4	-86 ± 5
$\beta^3\text{hGlu}^5$	-120 ± 8	-140 ± 8	49 ± 3	-58 ± 3
$\beta^3\text{hSer}^6$	-131 ± 7	-158 ± 8	74 ± 5	119 ± 57
$\beta^3\text{hTyr}^7$	-110 ± 7	-141 ± 5	35 ± 6	-122 ± 8
$\beta^3\text{hIle}^8$	-115 ± 8	–	102 ± 31	-41 ± 54

Table 6. *Statistics of Selected Dihedral Angles in the Structural Ensemble Calculated for β -Octapeptide 4.*
All 45 accepted structures were used. For definitions of dihedral angles, see Fig. 4.

	ϕ	ψ	θ	χ^1
$\beta^3\text{hVal}^1$	–	-155 ± 14	30 ± 37	-40 ± 36
$\beta^3\text{hLys}^2$	-147 ± 9	-136 ± 17	50 ± 6	-83 ± 11
$\beta^3\text{hSer}^3$	-137 ± 12	-136 ± 11	78 ± 8	40 ± 31
$\beta^3\text{hPhe}^4$	-141 ± 11	-147 ± 6	48 ± 8	-94 ± 1
$\beta^3\text{hGlu}^5$	-123 ± 8	-148 ± 5	56 ± 5	-61 ± 7
$\beta^3\text{hSer}^6$	-124 ± 4	-170 ± 6	71 ± 7	-129 ± 32
$\beta^3\text{hTyr}^7$	-112 ± 8	-144 ± 10	50 ± 17	-94 ± 38
$\beta^3\text{hIle}^8$	-128 ± 16	–	72 ± 19	31 ± 56

leads to the conclusion that the bridge in **4** does not distort the structure of this helix compared to **1**. The average $C_i^\beta \cdots C_{i+3}^\beta$ distance ('pitch' of the helix) is *ca.* 4.8 Å in both structures.

5. Conclusions and Discussion. – The $(\text{CH}_2)_4$ -hydrocarbon-tethered β -octapeptide derivative **4** and the non-restrained analog **1** have CD spectra (in MeOH and H₂O solution) which can be interpreted by assuming that there is 'more helicity' (*i.e.*, reduced conformational flexibility) caused by the covalently attached bridge in **4**. The origin of the trough near 215 nm in the CD spectra of β -peptides, the intensity of which is used for drawing this conclusion, is, however, controversial: the typical CD spectrum hardly changes when a MeOH solution of a β^3 -peptide⁸⁾ is heated to 60° and above [18a], or when it is treated with a 'denaturing' additive such as urea [18b]. On the other hand, addition of H₂O to MeOH solutions (or CD measurements in pure H₂O)⁹⁾ leads

8) ...consisting of *homologated, noncyclic, α -amino acid moieties*, and having a 3_1 -helical secondary structure by NMR analysis! The situation is different when *Gellman's cyclic β -amino-acid residues* (especially *ACHC*) are involved [1b–d][2d]. Also, when the β -peptide consists of 'disubstituted' $\beta^{2,3}$ -amino-acid residues of *like-configuration* [2c], the helix is very stable: in CD₃OD at r.t. the central NH H-atoms of a β -hexapeptide of this type [18i] undergo H/D exchange with a half-life of *ca.* 9 days!

9) The results of NMR measurements in H₂O, and of NMR titrations of MeOH solutions of the β -octapeptides **1** and **4** with H₂O will be reported and discussed in a forthcoming separate paper by our groups.

to a reduction [1c] or breakdown [18b,c] of the *Cotton* effect, or to a total change of the patterns of the spectra [15b,c][18d]. Furthermore, as mentioned above⁶), a ‘helix-typical’ CD spectrum is observed with β -peptides, which cannot possibly fold to a 3_{14} -helix. For these reasons we have always considered CD spectra of β -peptides as a mere qualitative kind of fingerprint.

The NMR solution-structure analysis of the two β^3 -octapeptides **1** and **4**, reported herein, was carried out with a precision (by including the complete set of side chain – side chain and side chain – backbone NOEs), which is unprecedented for β -peptides. While there are differences in the side-chain conformations with respect to salt-bridging between the Glu and Lys, or π -interaction between the Phe and Tyr side chains, the backbones of the two peptides are superimposable (*Fig. 5*) with an RMSD of 0.2 Å, which leads to the statement made above: ‘*the bridge in 4 does not distort the structure of this helix compared to 1*’, or in other words *no helix-stabilizing effect of the tether can be derived from the NMR analysis of the two peptides in MeOH*. The discrepancy between this conclusion and that drawn from the CD spectra suggests that the negative *Cotton* effect near 215 nm is actually not caused by the global nature of a single helical backbone conformation of the β -peptides but rather by the *local* extent of helicity also present in partially unfolded conformers.

In looking for an interpretation [2c][18e,f], one has to keep in mind that chemists very often tend to think in terms of static structures of molecules. Contrary to this view, most spectroscopic experiments are carried out on statistical ensembles. The ease, with which information from CD spectroscopy and from NOEs gained from an ensemble of molecules can be condensed into a single representative picture, depends, among others, on two factors, which are important for this discussion:

1. For an ensemble also consisting of partially unfolded macromolecules, a H...H distance derived from a NOE is likely to be biased towards smaller values, *i.e.*, towards the more compact members of the ensemble exhibiting strong NOEs¹⁰).

2. While the size of the *Cotton* effect represents a linear average from all contributing conformers, it is much more ‘shortsighted’ than NMR cross-relaxation experiments in the sense that it mainly reports on the local electronic structure and local conformation of the backbone.

As soon as more than one backbone conformation is populated to a significant extent, problems reconciling information derived from CD spectroscopy and NOEs in one ‘representative molecule’ are, therefore, likely to occur. Based on qualitative arguments, this is especially to be expected if the folding process is not cooperative, as it is presumably the case for the shorter β^3 -peptides [18a]¹¹).

To complement the data presented here, investigations aiming at the dynamics of the peptides **1** and **4** in aqueous media and in MeOH are in progress.

¹⁰) This is the result of the functional dependence of the NOE on the internuclear distance. The effect of angular fluctuations of the internuclear vectors is assumed to be negligible here.

¹¹) From investigations of F-substituted β^3 -hepta- and β^3 -tridecapeptides, we have recently concluded that longer-chain β^3 -peptides might be subject to cooperative folding [18g,h]. The central NH H-atom of a β^3 -pentadecapeptide has been found to undergo H/D exchange in CD₃OD at room temperature with a half-life of *ca.* 59 days, which is not compatible with dynamic opening and closing of H-bonds in this region of the peptide [18i]. Finally, for *Schepartz's* β -peptides (mostly dodecapeptides; *cf. Footnote 2*) cooperative behavior has also been reported [11c–h].

The authors wish to thank Dr. Denis Scanlon (Bio21 Institute, University of Melbourne) for access to HPLC purification facilities and Prof. Bernhard Jaun (ETH Zürich) for insightful discussions. J. G. acknowledges financial assistance from an ARC International Linkage Fellowship LX0881950, and A. D. A. support from ARC DP077190.

Experimental Part

1. *General Abbreviations*: DIPEA: EtN(i-Pr)₂, HATU: *O*-(7-azabenzotriazol-1-yl)-*N,N,N',N'*-tetraammonium hexafluorophosphate, HFIP: 1,1,1,3,3,3-hexafluoropropan-2-ol, TFA: CF₃COOH, h.v.: high vacuum (0.01 – 0.1 Torr), TNBS: 2,4,6-trinitrobenzenesulfonic acid, TIS: 2-Chlorotriethyl resin was purchased from GL Biochem (China). Fmoc-β³-amino acids were purchased from Fluka or prepared according to established procedures. Anal. reversed-phase (RP) HPLC: on an Agilent 1100 using a Supelco C₁₈ column (150 × 4.6 mm, 5 μm), using a linear gradient of A (MeCN) and B (0.1% TFA in H₂O) at a flow rate of 1 ml/min. Prep. HPLC: on an Agilent 1200 using an Agilent C₁₈ column (250 × 9.4 mm, 5 μm), using a linear gradient of A (MeCN) and B (0.1% TFA in H₂O) at a flow rate of 5 ml/min. Retention time (*t_R*) given in min. Lyophilization: Virtis benchtop SLC to obtain peptides as TFA salts. MS: Agilent 6510 QTOF LC/MS.

2. *Preparation of Peptides 1–4*. *H*-β³hVal-β³hLys-β³hSer(All)-β³hPhe-β³hGlu-β³hSer(All)-β³hTyr-β³hIle-OH (**1**). 2-Chlorotriethyl resin (150 mg, 0.8–1.5 mmol/g, ca. 0.17 mmol) was swollen in CH₂Cl₂ (5 ml) for 1 h. The resin was filtered, and a soln. of Fmoc-β³hIle-OH (121 mg, 0.33 mmol, 2 equiv.) and DIPEA (0.144 ml, 0.85 mmol, 5 equiv.) in CH₂Cl₂ (2 ml) was added and mixed under N₂ bubbling for 2 h. The resin was filtered, and the addition of Fmoc-β³hIle-OH was repeated once more for 2 h. The resin was filtered and washed with CH₂Cl₂ (5 ml, 5 × 1 min). The *N*-terminal Fmoc group was removed using 20% piperidine/DMF (4 ml, 4 × 10 min), and the resin was washed with DMF (5 ml, 5 × 1 min). The remaining Fmoc-protected β-amino acids were incorporated according to standard solid phase synthesis protocols with Fmoc-βAA-OH (2 equiv.), HATU (1.95 equiv.), and DIPEA (4 equiv.) as a soln. in DMF with a reaction time of 1 h: Fmoc-β³Tyr(tBu)-OH (174 mg), Fmoc-β³hSer(All)-OH (140 mg), Fmoc-β³hGlu(tBu)-OH (161 mg), Fmoc-β³hPhe-OH (148 mg), Fmoc-β³hSer(All)-OH (140 mg), Fmoc-β³hLys(Boc)-OH (177 mg), Fmoc-β³hVal-OH (130 mg); HATU (136 mg); DIPEA (0.128 ml). Couplings were monitored using TNBS [19]. Once the final residue was incorporated, the *N*-terminal Fmoc group was removed (20% piperidine/DMF, 4 ml, 4 × 10 min), and the resin was washed with DMF (5 ml, 5 × 1 min). A soln. of Boc₂O (157 mg, 0.72 mmol, 4.2 equiv.) and Et₃N (0.1 ml, 0.72 mmol, 4.2 equiv.) in CH₂Cl₂ (1 ml) was then added and mixed under N₂ bubbling for 1 h. The resin was filtered and washed with CH₂Cl₂ (5 ml, 5 × 1 min). The peptide–resin was then dried in h.v. for 12 h. A portion of the peptide–resin (50 mg) was treated with TFA/TIPS/H₂O (95:2.5:2.5, 10 ml) for 3 h. The resin was filtered, washed with TFA (2 × 2 ml), and the volatiles were removed under reduced pressure. The resulting residue was treated with cold Et₂O to precipitate the crude peptide (44 mg). Purification by prep. RP-HPLC (0–60% A in 25 min) gave **1** as TFA salt (5.5 mg). White solid. Anal. RP-HPLC (0–60% A in 25 min): *t_R* 19.7, >98%. HR-MS: 1164.6904 ([*M* + H]⁺, C₆₀H₉₄N₉O₁₄; calc. 1164.6920).

H-β³hVal-β³hLys-β³hSer(*X*)-β³hPhe-β³hGlu-β³hSer(*X*)-β³hTyr-β³hIle-OH (*X* = CH₂CH=CHCH₂ tether; **2**). A further portion of the peptide–resin from the preparation of **1** (200 mg) was treated with a soln. of HFIP/CH₂Cl₂ (3:7, 10 ml) for 30 min, filtered, and washed with CH₂Cl₂ (2 × 2 ml). The solns. were combined, and the volatiles were removed to give the fully protected linear peptide as a pale white solid (148 mg, LR-MS: 1475.9 (C₆₀H₉₄N₉O₁₄; calc. 1475.9). Grubbs' II ruthenium catalyst **5** (4 mg, 5 mol-%) was added to a soln. of the fully protected β-peptide (140 mg, 0.095 mmol) dissolved in degassed CH₂Cl₂ (5 ml) under N₂, and the mixture was stirred at 35° under N₂ for 2 h. An additional portion of catalyst was added, and stirring was continued for a further 2 h. The solvent was removed under reduced pressure to give the fully protected peptide as a light brown solid (145 mg, LR-MS: 1468 ([*M* + Na]⁺)). Treatment with TFA/TIS/H₂O (95:2.5:2.5, 5 ml) gave **2**. Light brown solid. HR-MS: 1136.6658 ([*M* + H]⁺, C₅₈H₉₀N₉O₁₄; calc. 1136.6607).

Fmoc-β³hVal-β³hLys-β³hSer(*X*)-β³hPhe-β³hGlu-β³hSer(*X*)-β³hTyr-β³hIle-OH (*X* = CH₂CH=CHCH₂ tether; **3**). Prepared in a similar manner as described for **2** except that the *N*-terminal Fmoc group of **1**

was not removed before cleavage of the peptide from the resin. Purification of a portion of the crude peptide (40 mg) by RP-HPLC (0–60%, in 40 min) gave **3** (5.6 mg). Grey solid. LR-MS: 1358 ($C_{73}H_{99}N_9O_{16}$; calc. 1358.6).

H- β^3 *hVal*- β^3 *hLys*- β^3 *hSer*(*X*)- β^3 *hPhe*- β^3 *hGlu*- β^3 *hSer*(*X*)- β^3 *hTyr*- β^3 *hIle-OH* (*X* = (CH₂)₄ tether; **4**). To a soln. of **2** (80 mg), dissolved in MeOH (2 ml) under N₂, was added 10% Pd/C (8 mg, 10% (w/w)), and the vessel was evacuated and flushed with H₂ (repeated 2 ×). The suspension was then vigorously stirred under H₂ for 3 h. The suspension was filtered through *Celite* (2-cm plug), and the solvent was removed to give a light brown solid (60 mg). Purification by prep. RP-HPLC (0–60% *A* in 25 min) gave pure **4** as a TFA salt (5.7 mg). White solid. Anal. RP-HPLC (0–60% *A* in 25 min): *t*_R 17.9, > 98%. LR-MS: 1137.6 ($C_{58}H_{91}N_9O_{14}$; calc. 1137.7).

3. *NMR Experiments*. All spectra were measured on a *Bruker AVANCE III* 600-MHz spectrometer at 26.4°. For both peptides, an identical set of spectra was acquired. The solvent signal was suppressed by presaturation. TOCSY and ¹³C-HSQC were run in a sensitivity-enhanced manner [20]. 80 ms of DIPSI2 isotropic mixing with a spin-lock field strength of 8.9 kHz was employed in the TOCSY experiments. Offset-compensated [21] ROESY spectra with 300-ms mixing time and a CW spin-lock field strength of 1.85 kHz were recorded. The spectral width was 5400 Hz in both dimensions. Quadrature detection in the indirect dimension was achieved by *States-TPPI*. 2k × 512 total data points were acquired. The time domain in both dimensions was extended to twice its size by zero-filling and apodized with a cos² function. The baseline of the resulting spectra was corrected with a polynomial of 5th order. All spectra were processed with Topspin 2.1 [22]. Resonance assignment, as well as integration and calibration of the ROESY cross-peaks and were performed with SPARKY 3.113 [23].

4. *Generation of Distance Restraints*. Two groups of cross-peaks for each peptide were used for calibration. Peptide **1**: *Ha*_{Si}/*Ha*_{Re} of residues 1–5 (peak group 1) and HN/HB of residues 2–8 (peak group 2); peptide **4**: *Ha*_{Si}/*Ha*_{Re} of all residues (peak group 1) and HN/HB of residues 2–8 (peak group 2). For both peptides, the average volume of peak group 1 and peak group 2 was assumed to correspond to distances of 1.9 and 2.9 Å, resp. These volumes and distances were used to solve the system of *Eqn. 1* for coefficients *a* and *b*, which were then used to generate distances from the remaining cross-peak volumes in the ROESY spectra.

$$r_{1,2} = a + b \cdot V_{1,2}^{-1/6} \quad (1)$$

The upper/lower limit of each restraint was generated by adding/subtracting 20% of the obtained distance. If a cross-peak could be integrated on both sides of the diagonal, the longer of the two resulting distances was used for structure calculation. Distances involving groups of equivalent protons (*e.g.*, Me groups) were multiplied by the corresponding correction factor *C* (*Eqn. 2*, where *n*₁ is the number of equivalent H-atoms in group I).

$$C = (n_I n_S)^{1/6} \quad (2)$$

In these cases, the restraint was implemented using an average distance *d* between the pairs of H-atoms involved (*Eqn. 3*).

$$d = ((d_{ij}^{-3})^{-1/3} \quad (3)$$

For cross-peaks involving diastereotopic H-atoms without stereospecific assignment, a similar procedure was employed. The longer of the two generated distances to a remote H-atom was introduced as a restraint on the average separation as defined in *Eqn. 3*. In these cases, the lower limit for the distance restraint was set to zero.

5. *Structure Calculation*. A simulated annealing protocol [24] implemented in XPLOR-NIH 2.21 [25] was employed to generate 45 structures for each peptide. The protocol consisted of 60 ps of high-temperature torsional angle molecular dynamics (TAD) at 20000 K, followed by 60 ps of slow cooling to 1000 K (TAD), 12 ps of slow cooling with Cartesian molecular dynamics to 300 K, and a final energy minimization in Cartesian coordinates. The only nonbonded interaction used was a repel potential. For each new structure, the starting velocities of all atoms were assigned randomly. A calculated structure

was accepted, if it showed no violation of a NOE restraint $> 0.2 \text{ \AA}$, no violation of a dihedral angle restraint $> 5^\circ$, no RMS deviation from the equilibrium values for bond lengths and bond angles $> 0.02 \text{ \AA}$ and $> 2^\circ$, resp., and no deviation from the equilibrium values of the impropers $> 1.5^\circ$. Topology and parameter files were adapted to accommodate β^3 -amino acid residues. The force constant for the stretching of a bond was $100 \text{ kcal mol}^{-1} \text{ \AA}^{-2}$, and the ones for angles and impropers were set to $500 \text{ kcal mol}^{-1} \text{ rad}^{-2}$.

Note added in proof: While the present paper was in print, an independent synthesis of hydrocarbon-chain-tethered β^3 -peptides by P. Perlmutter and his group was published [26]. For structural assignment, a couple of $3_{1,4}$ -helix-typical NOEs and CD-intensity comparisons were used.

REFERENCES

- [1] a) D. Seebach, M. Overhand, F. N. M. Kühnle, B. Martinoni, L. Oberer, U. Hommel, H. Widmer, *Helv. Chim. Acta* **1996**, *79*, 913; D. Seebach, P. E. Ciceri, M. Overhand, B. Jaun, D. Rigo, L. Oberer, U. Hommel, R. Amstutz, H. Widmer, *Helv. Chim. Acta* **1996**, *79*, 2043; b) D. H. Appella, L. A. Christianson, I. L. Karle, D. R. Powell, S. H. Gellman, *J. Am. Chem. Soc.* **1996**, *118*, 13071; c) D. Seebach, A. Jacobi, M. Rueping, K. Gademann, M. Ernst, B. Jaun, *Helv. Chim. Acta* **2000**, *83*, 2115, and in 'Hominatio – An International Tribute to Albert Eschenmoser', Ed. M. V. Kisakürek, Verlag Helvetica Chimica Acta, Zürich, Wiley-VCH, Weinheim, 2001; d) E. Vaz, W. C. Pomerantz, M. Geyer, S. H. Gellman, L. Brunsveld, *ChemBioChem* **2008**, *9*, 2254.
- [2] a) D. Seebach, J. Gardiner, *Acc. Chem. Res.* **2008**, *41*, 1366; b) D. Seebach, D. F. Hook, A. Glattli, *Biopolymers* **2006**, *84*, 23; c) D. Seebach, A. K. Beck, D. J. Bierbaum, *Chem. Biodiversity* **2004**, *1*, 1111; d) R. P. Cheng, S. H. Gellman, W. F. DeGrado, *Chem. Rev.* **2001**, *101*, 3898; e) D. Seebach, J. L. Matthews, *Chem. Commun.* **1997**, 2015.
- [3] L. K. Henschley, A. J. Jochim, P. S. Arora, *Curr. Opin. Chem. Biol.* **2008**, *12*, 692; J. Garner, M. M. Harding, *Org. Biomol. Chem.* **2007**, *5*, 3577.
- [4] N. E. Shepherd, G. Abbenante, D. P. Fairlie, *Angew. Chem.* **2004**, *116*, 2741; *Angew. Chem., Int. Ed.* **2004**, *43*, 2687; P. Grieco, P. M. Gitu, V. J. Hrubby, *J. Pept. Res.* **2001**, *57*, 250; K. A. Carpenter, R. Schmidt, S. Y. Yue, L. Hodzic, C. Pou, K. Payza, C. Godbout, W. Brown, E. Roberts, *Biochemistry* **1999**, *38*, 15295.
- [5] S. Cantel, A. Le Chavalier Isaad, M. Scrima, J. J. Levy, R. D. DiMarchi, P. Rovero, J. A. Halperin, A. M. D'Ursi, A. M. Papini, M. Chorev, *J. Org. Chem.* **2008**, *73*, 5663.
- [6] A. K. Boal, I. Guryanov, A. Moretto, M. Crisma, E. L. Lanni, C. Toniolo, R. H. Grubbs, D. J. O'Leary, *J. Am. Chem. Soc.* **2007**, *129*, 6986; H. E. Blackwell, R. H. Grubbs, *Angew. Chem.* **1998**, *110*, 3469; *Angew. Chem., Int. Ed.* **1998**, *37*, 3281.
- [7] Y.-W. Kim, G. L. Verdine, *Bioorg. Med. Chem. Lett.* **2009**, *19*, 2533; F. Bernal, A. F. Tyler, S. J. Korsmeyer, L. D. Walensky, G. L. Verdine, *J. Am. Chem. Soc.* **2007**, *129*, 2456; L. D. Walensky, K. Pitter, J. Morash, K. J. Oh, S. Barbuto, J. Fisher, E. Smith, G. L. Verdine, S. J. Korsmeyer, *Mol. Cell* **2006**, *24*, 199; L. D. Walensky, A. L. Kung, I. Escher, T. J. Malia, S. Barbuto, R. D. Wright, G. Wagner, G. J. Verdine, S. J. Korsmeyer, *Science* **2004**, *305*, 1466; C. E. Schafmeister, J. Po, G. L. Verdine, *J. Am. Chem. Soc.* **2000**, *122*, 5891.
- [8] M. A. Hossain, K. J. Rosengren, S. Zhang, R. A. D. Bathgate, G. W. Tregear, B. J. van Lierop, A. J. Robinson, J. D. Wade, *Org. Biomol. Chem.* **2009**, *7*, 1547; A. J. Robinson, J. Elaridi, B. J. van Lierop, S. Mujcinovic, W. R. Jackson, *J. Pept. Sci.* **2007**, *13*, 280.
- [9] A. J. Vernall, P. Cassidy, P. F. Alewood, *Angew. Chem.* **2009**, *121*, 5785; *Angew. Chem., Int. Ed.* **2009**, *48*, 5675; D. Wang, W. Liao, P. S. Arora, *Angew. Chem.* **2005**, *117*, 6683; *Angew. Chem., Int. Ed.* **2005**, *44*, 6525; E. Cabezas, A. C. Satterthwait, *J. Am. Chem. Soc.* **1999**, *121*, 3862.
- [10] D. H. Appella, J. J. Barchi Jr., S. R. Durell, S. H. Gellman, *J. Am. Chem. Soc.* **1999**, *121*, 2309.
- [11] a) P. I. Arvidsson, M. Rueping, D. Seebach, *Chem. Commun.* **2001**, 649; b) R. P. Cheng, W. F. DeGrado, *J. Am. Chem. Soc.* **2001**, *123*, 5162; c) S. A. Hart, A. B. F. Bahadoor, E. E. Matthews, X. J. Qiu, A. Schepartz, *J. Am. Chem. Soc.* **2003**, *125*, 4022; d) J. A. Kritzer, J. Tirado-Rives, S. A. Hart,

- J. D. Lear, W. L. Jorgensen, A. Schepartz, *J. Am. Chem. Soc.* **2005**, *127*, 167; e) J. X. Qiu, E. J. Petersson, E. E. Matthews, A. Schepartz, *J. Am. Chem. Soc.* **2006**, *128*, 11338; f) D. S. Daniels, E. J. Petersson, J. X. Qiu, A. Schepartz, *J. Am. Chem. Soc.* **2007**, *129*, 1532; g) E. J. Petersson, A. Schepartz, *J. Am. Chem. Soc.* **2008**, *130*, 821; h) J. L. Goodman, M. A. Molski, J. Qiu, A. Schepartz, *ChemBioChem* **2008**, *9*, 1576.
- [12] M. Rueping, B. Jaun, D. Seebach, *Chem. Commun.* **2000**, 2267; A. Jacobi, D. Seebach, *Helv. Chim. Acta* **1999**, *82*, 1150.
- [13] E. Vaz, L. Brunsveld, *Org. Lett.* **2006**, *8*, 4199.
- [14] Y. Bergman, M. Ciampini, S. Jalal, H. R. Lagiakos, M.-I. Aguilar, P. Perlmutter, *Tetrahedron: Asymmetry* **2008**, *19*, 2861.
- [15] a) D. Seebach, T. Sifferlen, P. A. Mathieu, A. M. Häne, C. M. Krell, D. J. Bierbaum, S. Abele, *Helv. Chim. Acta* **2000**, *83*, 2849; b) J. V. Schreiber, D. Seebach, *Helv. Chim. Acta* **2000**, *83*, 3139; c) D. Seebach, J. V. Schreiber, P. I. Arvidsson, J. Frackenpohl, *Helv. Chim. Acta* **2001**, *84*, 271; d) A. Glättli, X. Daura, D. Seebach, W. F. van Gunsteren, *J. Am. Chem. Soc.* **2002**, *124*, 12972; e) X. Daura, D. Bakowies, D. Seebach, J. Fleischhauer, W. F. van Gunsteren, P. Krüger, *Eur. Biophys. J.* **2003**, *32*, 661.
- [16] D. S. Kemp, *Helv. Chim. Acta* **2002**, *85*, 4392.
- [17] A. C. Wang, A. Bax, *J. Am. Chem. Soc.* **1996**, *118*, 2483.
- [18] a) K. Gademann, B. Jaun, D. Seebach, R. Perozzo, L. Scapozza, G. Folkers, *Helv. Chim. Acta* **1999**, *82*, 1; b) T. Etezardy-Esfarjani, C. Hilty, K. Wüthrich, M. Rueping, J. Schreiber, D. Seebach, *Helv. Chim. Acta* **2002**, *85*, 1197; c) S. Abele, G. Guichard, D. Seebach, *Helv. Chim. Acta* **1998**, *81*, 2141; d) D. Seebach, T. Kimmmerlin, R. Šebesta, M. A. Campo, A. K. Beck, *Tetrahedron* **2004**, *60*, 7455; e) J. Kapitán, F. Zhu, L. Hecht, J. Gardiner, D. Seebach, L. D. Barron, *Angew. Chem.* **2008**, *120*, 6492; *Angew. Chem., Int. Ed.* **2008**, *47*, 6392; f) D. Seebach, H. Widmer, S. Capone, R. R. Ernst, T. Bremi, I. Kieltsch, A. Togni, D. Monna, D. Langenegger, D. Hoyer, *Helv. Chim. Acta* **2009**, *92*, in print, doi: 10.1002/hlca.200900279; g) R. I. Mathad, B. Jaun, O. Flögel, J. Gardiner, M. Löweneck, J. D. C. Codée, P. H. Seeberger, D. Seebach, M. K. Edmonds, F. H. M. Graichen, A. D. Abell, *Helv. Chim. Acta* **2007**, *90*, 2251; h) R. I. Mathad, F. Gessier, D. Seebach, B. Jaun, *Helv. Chim. Acta* **2005**, *88*, 266; i) D. Seebach, S. Abele, K. Gademann, G. Guichard, T. Hintermann, B. Jaun, J.-L. Matthews, J. V. Schreiber, L. Oberer, U. Hommel, H. Widmer, *Helv. Chim. Acta* **1998**, *81*, 932.
- [19] W. S. Hancock, J. E. Battersby, *Anal. Biochem.* **1976**, *71*, 260.
- [20] A. G. Palmer III, J. Cavanagh, P. E. Wright, M. Rance, *J. Magn. Reson.* **1991**, *93*, 151; J. Cavanagh, M. Rance, *J. Magn. Reson.* **1990**, *88*, 72.
- [21] C. Griesinger, R. R. Ernst, *J. Magn. Reson.* **1987**, *75*, 261.
- [22] Bruker Biospin GmbH, Reinstetten, 2007.
- [23] T. D. Goddard, D. G. Kneller, University of California, San Francisco, 2004.
- [24] E. G. Stein, L. M. Rice, A. T. Brünger, *J. Magn. Reson.* **1997**, *124*, 154.
- [25] C. D. Schwieters, J. J. Kuszewski, N. Tjandra, G. M. Clore, *J. Magn. Reson.* **2003**, *160*, 66.
- [26] Y. E. Bergman, M. P. Del Borgo, R. D. Gopalan, S. Jalal, S. E. Unabia, M. Ciampini, D. J. Clayton, J. M. Fletcher, R. J. Mulder, J. A. Wilce, M.-I. Aguilar, P. Perlmutter, *Org. Lett.* **2009**, *11*, 4438.

Received August 31, 2009